OPEN ACCESS

University of BRISTOL

Clements, T., Dolocan, A., Martin, P. G., Purnell, M. A., Vinther, J., & Gabbott, S. E. (2016). The eyes of Tullimonstrum reveal a vertebrate affinity. Nature, 532, 500-503. DOI: 10.1038/nature17647

Peer reviewed version

License (if available):
Other

Link to published version (if available):
10.1038/nature17647

Link to publication record in Explore Bristol Research
PDF-document

University of Bristol - Explore Bristol Research

General rights

This document is made available in accordance with publisher policies. Please cite only the published version using the reference above. Full terms of use are available:
http://www.bristol.ac.uk/pure/about/ebr-terms.html

Eyes of *Tullimonstrum gregarium* (Mazon Creek, Carboniferous) reveal a vertebrate affinity

Thomas Clements[1], Andrei Dolocan[2] Peter Martin[3,4], Mark A. Purnell[1], Jakob Vinther[3,5,*] & Sarah E. Gabbott[1*]

[1]Department of Geology, University of Leicester, Leicester, LE1 7RH, UK

[2]Texas Materials Institute, The University of Texas at Austin, Austin, TX 78712, USA

[3]School of Earth Sciences, University of Bristol, Bristol, BS8 1RJ, UK

[4]Interface Analysis Centre, HH Wills Physics Laboratory, University of Bristol, Bristol, BS8 1TQ, UK

[5]School of Biological Sciences, University of Bristol, Bristol, BS8 1TQ, UK

*Corresponding authors

Tullimonstrum gregarium **is an iconic soft-bodied fossil from the Carboniferous Mazon Creek Lagerstätte (Illinois)[1]. Despite a large number of specimens and distinct anatomy, various analyses over the last five decades have failed to determine the phylogenetic affinities of the "Tully Monster", and although it has been allied to such disparate phyla as the Mollusca[2], Annelida[3,4] or Chordata[5], it remains enigmatic[1-5]. The nature and phylogenetic affinities of *Tullimonstrum* have defied confident systematic placement because none of its preserved anatomy provides unequivocal evidence of homology, without which comparative analysis fails. Here we show that the eyes of *Tullimonstrum* possess ultrastructural details indicating homology with vertebrate eyes. Anatomical analysis using scanning electron microscopy reveals that the eyes of *Tullimonstrum* preserve a retina defined by a thick sheet comprising distinct layers**

of spheroidal and cylindrical shaped melanosomes. Time of Flight Secondary Ion Mass Spectrometry (TOF-SIMS) provides further evidence for microbodies being melanosomes. A range of animals have melanin in their eyes, but the possession of melanosomes of two distinct morphologies arranged in layers, forming reticulated pigmented epithelium (RPE), is a synapomorphy of vertebrates. Our analysis indicates that in addition to evidence of colour patterning[6], ecology[7] and thermoregulation[8], fossil melanosomes can also carry a phylogenetic signal. Identification in *Tullimonstrum* of spheroidal and cylindrical melanosomes forming the remains of RPE indicates that it is a vertebrate; considering its body parts in this new light suggests it was an anatomically unusual member of total group Vertebrata.

The enigmatic *Tullimonstrum gregarium* from the Carboniferous Mazon Creek Lagerstätte (307 Ma) is among the world's most notorious fossils. Familiar to millions of people as the state fossil of Illinois, reconstructions of the "Tully Monster" have graced the sides of U-Haul™ trailers across the USA. Yet the phylogenetic affinity of *Tullimonstrum* remains unresolved. In contrast with the Cambrian Chengjiang and Burgess Shales biotas, the Mazon Creek preserves fossils which are largely familiar (at least at the level of higher taxa) with *Tullimonstrum* being a notable anomaly in this respect. *Tullimonstrum*, a monotypic taxon, known from several hundred specimens, is preserved as stains with some relief within Mazon Creek siderite nodules. Despite the uncertainty about its position in the tree of life, there is a surprisingly high level of agreement regarding the arrangement and shape of anatomical features (Fig. 1). The anatomical complexity, evident cardinal axes and the bilateral symmetry demonstrates that *Tullimonstrum* is a bilaterian[1-3,5] but beyond this, it has defied systematic placement. Given the consensus regarding the shape and anatomical disposition of body parts this might seem perplexing but the issue is in fact quite simple: there is little agreement about its affinities because no study has identified unequivocal homologies/synapomorphies upon which to base a solid comparative anatomical interpretation. This is a classic example of how, without the criterion of topological relations

between body parts as a potential falsifier of character hypotheses, testing of alternative hypotheses becomes problematic[9,10]. Different choices of extant anatomical comparator result in radically different hypotheses of homology and affinity for *Tullimonstrum* (Fig. 1) but evidence to test which hypothesis is correct remains elusive. Where topological data in fossils are equivocal, other homology criteria, normally subordinate to topology assume greater importance[9-11]. Here we apply the criterion of the intrinsic properties of body parts (also referred to as 'special qualities''[10] or 'correspondence of composition'[11]) allowing us to resolve the phylogenetic placement of *Tullimonstrum.*

One of the defining characters of *Tullimonstrum* is the transverse bar. Associated with this in many specimens is a pair of dark structures which, regardless of the orientation of the fossil, occur at the distal ends of the bar (Figs 1-2; Extended Data Fig. 1). The transverse bar is relatively straight, although it bends forwards or backwards in some specimens[3]; it is preserved in relief, suggesting a relatively recalcitrant structure, but there is no evidence that it was biomineralised[3]. Scanning electron microscopy, TOF-SIMS and EDS reveals that the dark structures comprise thick, multi-layered masses of tightly-packed, micron-sized bodies composed of carbonaceous material (Fig. 2). They exhibit two distinct morphologies: highly cylindrical forms with rounded terminations (1.3 - 2.0 µm long and 0.3 - 0.4 µm wide), and oblate, almost spherical forms (0.4 - 0.7 µm diameter). There are at least two layers of bodies, with oblate and cylindrical types showing little intermixing (Fig. 2; Extended Data Fig. 1). No other anatomy, even that composed of carbon, exhibits this microtexture (Extended Data Fig. 2).

The composition, anatomical localisation and fabrics indicate that the cylindrical and oblate bodies are layers of melanosomes; the range of shape and size compares closely with extant and fossilised melanosomes[6]. To further test this hypothesis we employed TOF-SIMS analysis and principal component analysis (PCA) to compare the relative intensity distribution of the melanin-specific peaks originating from fresh, artificially matured, fossil melanin and non-melanin samples (Extended Data Fig. 3). Direct comparison of spectra

from *Tullimonstrum* and pure melanin samples[8,12] shows a similar spectral composition (Fig. 3, Extended Data Fig. 4). PCA shows *Tullimonstrum* data plot among samples of fossil melanin[13] (Fig. 3, Extended Data Fig. 3), thus providing, in addition to anatomical localization and morphology, independent evidence that the microbodies are melanosomes. An alternative interpretation is that microbodies are the remains of melanin synthesising bacteria or fungi. This scenario is unlikely because these microorganisms are not known to colonise decaying bodies, and their distribution in the fossils would require that they localised only to formerly melanin synthesising tissues.

Within the Mazon Creek Lagerstätte the only other fossils to possess paired, dark, ovoid structures are the numerous vertebrates (cyclostomes and gnathostomes), and a single putative coleoid[12]. In vertebrates, anatomical landmarks indicate that the dark structures are eyes (e.g.[13-16] and Extended Data Fig. 5). Eyes in basal vertebrates are relatively decay resistant[17,18] and pigment is one of the most decay resistant features in lampreys[17,18]. In *Tullimonstrum,* the dark structures are paired, bilaterally disposed and comprise thick, multi-layered masses of melanosomes. Together, these data constitute strong evidence that the dark structures are eyes.

Retinal pigments function as visual photoreceptors or as screening pigments that act to prevent stray light from reaching the photoreceptive cells[19]. Whilst all metazoans can synthesise melanin, ocular screening pigments are known to vary, and current data indicates that invertebrates chiefly employ ommochromes and pterines[20]. In annelids, molluscs, and arthropods evidence indicates that these pigments are contained in microbodies that are exclusively spherical or slightly oval, frequently facetted by abutting pigment granules and cell walls. There are a handful of invertebrate groups where melanin has been chemically identified as the screening pigment (planarian flatworms[21], cubozoan cnidarians[22] and ascidians[23], phaeomelanin in the shell eyes of chitons[24]). Significantly, the available ultrastructural data indicates that where these groups employ melanin, their melanosomes are exclusively ovoid (Fig. 4; see also Supplementary Information).

Chordates are unusual among metazoans in that their ocular screening pigments are exclusively melanin[22]. In vertebrate eyes, the iris, choroid and retinal pigmented epithelium (RPE) all contain melanosomes but the latter tissue is distinct in having layers of ovoid *and* cylindrical melanosomes[25]. *Tullimonstrum* eyes comprise ovoid and cyclindrical melanosomes that occur in distinct layers (i.e. not intermixed; Fig. 2 and Extended Data Fig. 1) and we therefore interpret the melanosome layer as the remains of RPE. The possibility that this micro-anatomical complex – melanosomes of the same size and shape, arranged in layers, exclusively in the eye – was convergently acquired by *Tullimonstrum* and vertebrates is non-parsimonious. Based on the available evidence from extant animals this character complex is a synapomorphy of vertebrates, and it thus represents an unequivocal phylogenetically informative homology in *Tullimonstrum*.

The homology of RPE in *Tullimonstrum* provides the phylogenetic context for comparative anatomical evaluation. A full analysis, including comparative taphonomy, is beyond the scope of this contribution, but here we consider the main body parts (Fig. 1) particularly diagnostic characters of the Chordata such as the notochord and myomeres.

Of the generally accepted body parts in *Tullimonstrum* none is readily interpreted as a notochord or a branchial structure. Fossil lamprey and hagfish (i.e. nonbiomineralised vertebrates), from the Mazon Creek also lack a preserved notochord[13,14] suggesting that absence in *Tullimonstrum* is likely to reflect a failure to fossilise rather than an absence from the organism. Similarly, branchial structures of Mazon Creek lampreys and hagfish are preserved in a way that indicates they were pigmented in life (pers obs); we take their absence from *Tullimonstrum* to indicate that they were unpigmented. V-shaped stains interpreted as myomeres are known from Mazon Creek agnathans (e.g.[26]), and the hypothesis that the transverse sigmoidal bands of the trunk in *Tullimonstrum* represent myomeres or myosepta is certainly possible. The asymmetrical, oblanceolate posterior fins of *Tullimonstrum* have generally been reconstructed as dorso-ventrally flattened[3], and this would be unusual in a vertebrate. However, analysis indicates that the tail was laterally-

flattened in life and that the apparent dorso-ventral flattening in some specimens is a result of post-mortem twisting, evidenced by oblique wrinkles commonly seen in the posterior portion of the body immediately anterior to the tail[2,5], also commonly seen in Mazon Creek chondrichthyans[15]. So *Tullimonstrum*, when considered through a taphonomic filter, does preserve some features consistent with a vertebrate body plan.

The most perplexing features of *Tullimonstrum* are the proboscis-like anterior, terminating in a claw-like structure, and the transverse bar. The former remains contentious as it is difficult to determine whether the distal end is a buccal mass[2], a grasping claw[3], or a flexible proboscis. Under a vertebrate model, the 'stylets' could represent biomineralised teeth or dermal denticles, and this is consistent with their mouldic preservation, comparable to biomineralised structures in Mazon Creek gnathostomes[16]. If the 'claw' is a buccal mass this might reflect anterior rostralisation or posterior displacement of the eye. Perhaps more likely is the interpretation of this flexible rostral extension as a proboscis, similar to that of the Australian ghost shark *Callorhinchus milii* (Holocephali). The unusual transverse bar we interpret as a stalked eye structure, based on the presence of melanosomes and the remains of RPE. Stalked eyes occur in several animal groups including vertebrates, with larvae of several phylogenetically distinct teleost clades possessing eyes borne on stalks, up to one-quarter the length of the body[27]. The larvae of *Idiacanthus fasciola*[27] and *Stylopthalmus paradoxus*, for example, resemble *Tullimonstrum* in having markedly stalked eyes and a rostral extension. Stalked eyes with well-developed RPE (and a possible lens see Fig. 2; Extended Data Fig. 1) suggests a camera style eye capable of image formation, meaning that vision in *Tullimonstrum* involved more than simple detection of light direction as is the case in non-vertebrate chordates.

None of the preserved anatomy of *Tullimonstrum* contradicts the hypothesis that it is a vertebrate, and in the absence of any other unequivocal indicators of homology we show that the intrinsic properties of the eye, a character complex indicative of vertebrate RPE, provides compelling evidence that *Tullimonstrum* is a total group vertebrate. A dual-

melanosome RPE evolved at some stage along the vertebrate stem and therefore does not constrain how near the base of the vertebrate tree *Tullimonstrum* might sit. However, if this type of RPE is a synapomorphy of crown vertebrates, and the stylets in the 'claw' prove to be the remains of biomineralised (phosphatised) structures, the affinities of *Tullimonstrum* would lie with total group gnathostomes. Lacking any evidence of a bony skeleton, a placement within Osteichthyes is unlikely, but without additional diagnostic characters *Tullimonstrum* cannot presently be assigned to any more specifically delineated clade.

Methods

As part of a larger study on pigment preservation and taphonomy in the Mazon Creek, we investigated the dark elliptical patches at the terminations of the transverse bar in 12 specimens of *Tullimonstrum gregarium* from the Burpee Museum of Natural History, Illinois and the Field Museum of Natural History, Illinois. We analysed textural and compositional data using a Hitachi S-3600N and Zeiss Sigma Environmental Scanning Electron Microscope with EDX system. Partial pressure was 20-30 Pa, working distance was between 9-12 mm, with an operating voltage of 15 kV. Specimens were uncoated. Specimens were optically imaged, using a Canon Eos5 dSLR camera and a Leica M205c stereo microscope.

For TOF-SIMS analysis, one of the eyes in MCPX27C5369 (Burpee Museum of Natural History) was used. The specimen was placed in a TOF-SIMS 5 (ION-TOF GmbH, 2010) and secondary ion spectra were collected using a polyatomic analysis beam (Bi_3+, 30 keV, 0.9 pA sample current) to increase the yield of organic fragments, as previously employed by Colleary *et al.*[28]. Two 500 x 500 μm^2 areas were analysed in negative polarity with a resolution of 512 x 512 pixels: one area included the eye and adjacent matrix, another region was selected within the main body of the eye. The acquired spectrum from within the eye showed no significant effect of topography and was analysed without further processing, while a region of interest was chosen from the sampled area of the eye and sediment

spectrum to minimise topographic-related artefacts. All spectra were mass calibrated using the polyatomic fragment series of carbon (C-, C_2-, C_3-, C_4-, C_5-, C_7-, C_8-, C_9-, C_{10}-). The total count intensities of 55 select secondary ion peaks representative for melanin were used for PCA in conjunction with a previously collected dataset[28] of artificially matured melanin. Prior to PCA, each melanin-specific spectrum is normalized to its total intensity, the resulting dataset is mean-centred and then standard-deviation-normalised across all samples for each composing mass. The latter process ensures that each melanin-specific peak is given the same weight in the PCA. The *Tullimonstrum* spectra are shown alongside extant reference melanin samples: black (eu)melanosomes from a glossy Carion Crow, *Corvus corone* (Fig. 3b, Extended Data Fig. 4) and reddish brown domestic chicken, *Gallus gallus* (Extended Data Fig. 4) as well as representative fossil samples, that is, Jurassic ink sac and Eocene frog eye (Extended Data Fig. 4). Spatial mapping of the melanin-characteristic fragments of the melanosomes within the eye region show a clear separation at micron level between the cement (Extended Data Fig. 6e-h) and sediment (Extended Data Fig. 6i-l,u-x), while certain inorganic ions, attributed to calcium phosphates occur associated with the melanosomes (Extended Data Fig. 6 q-t).

1 Richardson, E. S. Wormlike fossil from the Pennsylvanian of Illinois. *Science* **151**, 75-76 (1966).

2 Foster, M. & Nitecki, M. A reappraisal of Tullimonstrum gregarium. *Mazon Creek fossils (ed. MH Nitecki)*, 269-301 (1979).

3 Johnson, R. G. & Richardson, E. S. Pennsylvanian invertebrates of the Mazon Creek Area, Illinois: the morphology and affinities of Tullimonstrum. *Fieldiana Geology* **12**, 119 -149 (1969).

4 Schram, F. Cladistic analysis of metazoan phyla and the placement of fossil problematica. *The early evolution of Metazoa and the significance of problematic taxa*, 35-46 (1991).

5 Beall, B. The Tully Monster and a new approach to analyzing problematica. *The early evolution of metazoa and the significance of problematic taxa (AM Simonetta and S. Conway Morris, eds.). Cambridge Univ. Press, Cambridge, England*, 217-186 (1991).

6 Vinther, J., Briggs, D. E., Prum, R. O. & Saranathan, V. The colour of fossil feathers. *Biology Letters* **4**, 522-525 (2008).

7 Clarke, J. A. *et al.* Fossil evidence for evolution of the shape and color of penguin feathers. *Science* **330**, 954-957 (2010).

8 Lindgren, J. *et al.* Skin pigmentation provides evidence of convergent melanism in extinct marine reptiles. *Nature* **506**, 484-488 (2014).

9 Donoghue, P. C. & Purnell, M. A. Distinguishing heat from light in debate over controversial fossils. *Bioessays* **31**, 178-189 (2009).

10 Rieppel, O. & Kearney, M. Similarity. *Biological Journal of the Linnean Society* **75**, 59-82 (2002).
11 Ruppert, E. E. Key characters uniting hemichordates and chordates: homologies or homoplasies? *Canadian journal of zoology* **83**, 8-23 (2005).
12 Kluessendorf, J. & Doyle, P. Pohlsepia mazonensis, an early 'octopus' from the Carboniferous of Illinois, USA. *Palaeontology* **43**, 919-926 (2000).
13 Bardack, D. First fossil hagfish (Myxinoidea): a record from the Pennsylvanian of Illinois. *Science* **254**, 701-703 (1991).
14 Bardack, D. & Zangerl, R. First fossil lamprey: a record from the Pennsylvanian of Illinois. *Science* **162**, 1265-1267 (1968).
15 Sallan, L. C. & Coates, M. I. The long-rostrumed elasmobranch Bandringa Zangerl, 1969, and taphonomy within a Carboniferous shark nursery. *Journal of Vertebrate Paleontology* **34**, 22-33 (2014).
16 Shabica, C. W. & Hay, A. *Richardson's guide to the fossil fauna of Mazon Creek*. (Northeastern Illinois University, 1997).
17 Sansom, R. S., Gabbott, S. E. & Purnell, M. A. Decay of vertebrate characters in hagfish and lamprey (Cyclostomata) and the implications for the vertebrate fossil record. *Proceedings of the Royal Society of London B: Biological Sciences* **278**, 1150-1157 (2011).
18 Sansom, R. S., Gabbott, S. E. & Purnell, M. A. Atlas of vertebrate decay: a visual and taphonomic guide to fossil interpretation. *Palaeontology* **56**, 457-474 (2013).
19 Fein, A. & Szuts, E. Z. *Photoreceptors, their role in vision*. Vol. 5 (CUP Archive, 1982).
20 Vopalensky, P. & Kozmik, Z. Eye evolution: common use and independent recruitment of genetic components. *Philosophical Transactions of the Royal Society B: Biological Sciences* **364**, 2819-2832 (2009).
21 Hase, S. *et al.* Characterization of the pigment produced by the planarian, Dugesia ryukyuensis. *Pigment cell research* **19**, 248-249 (2006).
22 Kozmik, Z. *et al.* Assembly of the cnidarian camera-type eye from vertebrate-like components. *Proceedings of the National Academy of Sciences* **105**, 8989-8993 (2008).
23 Sato, S. & Yamamoto, H. Development of pigment cells in the brain of ascidian tadpole larvae: insights into the origins of vertebrate pigment cells. *Pigment Cell Research* **14**, 428-436 (2001).
24 Speiser, D. I., DeMartini, D. G. & Oakley, T. H. The shell-eyes of the chiton Acanthopleura granulata (Mollusca, Polyplacophora) use pheomelanin as a screening pigment. *Journal of Natural History* **48**, 2899-2911 (2014).
25 Liu, Y. *et al.* Comparisons of the Structural and Chemical Properties of Melanosomes Isolated from Retinal Pigment Epithelium, Iris and Choroid of Newborn and Mature Bovine Eyes. *Photochemist. & Photobiol.* **81**, 510-516 (2005).
26 Bardack, D. & Richardson Jr, E. New agnathous fishes from the Pennsylvanian of Illinois. *Fieldiana* **33**, 489-510 (1977).
27 Weihs, D. & Moser, H. Stalked eyes as an adaptation towards more efficient foraging in marine fish larvae. *Bulletin of Marine Science* **31**, 31-36 (1981).
28 Colleary, C. *et al.* Chemical, experimental, and morphological evidence for diagenetically altered melanin in exceptionally preserved fossils. *PNAS* (2015).
29 Haacke, C., Heß, M., Melzer, R. R., Gebhart, H. & Smola, U. Fine structure and development of the retina of the grenadier anchovy Coilia nasus (Engraulididae, Clupeiformes). *Journal of morphology* **248**, 41-55 (2001).

Acknowledgments. William Simpson, Paul Mayer (Chicago Field Museum), Scott Williams (Burpee Museum of Natural History), David Rudkin and Kevin Seymour (Royal Ontario Museum) are thanked for specimen access and loans. Funded through Natural Environment

Research Council studentship P14DF19 (T.C.) and grant NE/K004557/1 (M.A.P and S.E.G.). We also acknowledge the NSF grant DMR-0923096 used to purchase the TOF-SIMS instrument at Texas Materials Institute, UTA. Duncan Murdock, Sophie Wentges and Amanda Clements are thanked for proof reading. Steve Furzeland (Zeiss) is thanked for SEM optimization. Phil Smith is thanked for AI tutorials.

Author contributions S.E.G, J.V. and T.C. designed and performed research. S.E.G and M.A.P conceived the research programme of which this work is part. S.E.G, T.C., J.V., M.A.P. and A.D. wrote the manuscript. A.D. and J.V. undertook TOF-SIMs analyses and interpretation. J.V. A.D. and M.A.P. conducted PCA analyses. S.E.G., J.V. and P.M. operated and optimised the SEM.

Authors for correspondence: Sarah E. Gabbott (sg21@le.ac.uk) & Jakob Vinther (jv12351@bristol.ac.uk).

Figures:

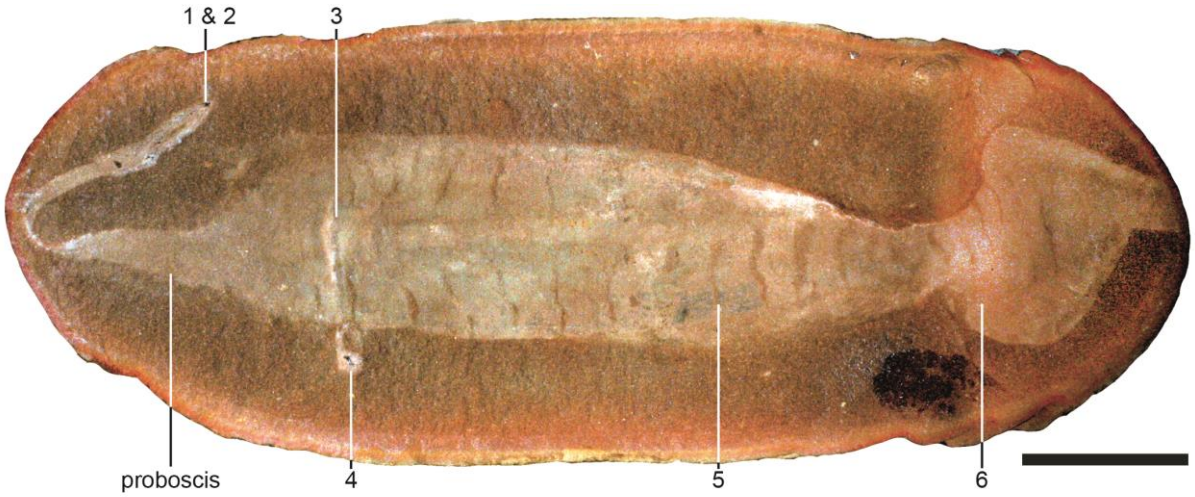

	1 Termination of appendage	2 Stylets in terminal structure	3 Transverse bar	4 Distal structures on transverse bar	5 Transverse sigmoidal bands on trunk	6 Extentions to posterior body outline	Proposed affinity
Ricardson (1966)	Jaw apparatus	Stylets/teeth	N/A	Bar organs	Segmentation	Lateral tail fins	*Incertae sedis*
Johnson & Ricardson (1966)	Grasping claw Jaw	Stylets	Sensory organs Otocysts Hydrodynamic stabilisers	Eyes	Segmentation	Lateral tail fins	Nemertea Polychaeta Sipunculidea Arthropoda Echiuroidea
Foster (1979)	Buccal mass	Teeth	Eye stalks	Eyes	Segmentation Muscle bands	Lateral tail fins Dorso-ventral tail fins	Nemertea Polychaeta Mollusca
Beall (1991)	Grasping claw Jaw Buccal mass	Teeth	Paired copulatory organs Setae	N/A	Segmentation Muscle bands	Dorso-ventral tail fins	Mollusca Conodonta
Schram (1991)	N/A	N/A	N/A	N/A	Segmented muscles	Caudal appendage	Nemertea Annelida
Proposed herein:	Buccal mass	Teeth or Dermal denticles	Eye stalks	Eyes	Myomeres?	Dorso-ventral tail fins	Non-osteichthyan gnathostome

Figure 1 | Interpretations of anatomy and affinity of *Tullimonstrum gregarium* from the Mazon Creek Lagerstätte. a, Optical image (BMRP2014MCP1000) showing typical morphology and spatial relationships between the principal anatomical features. Scale bar: 40 mm. **b,** Table showing interpretations of the anatomy and affinity of *Tullimonstrum*. 'Proposed affinity' lists the range of groups that *Tullimonstrum* has been allied to. Underlined groups indicate the phylogenetic placement favoured in each original study.

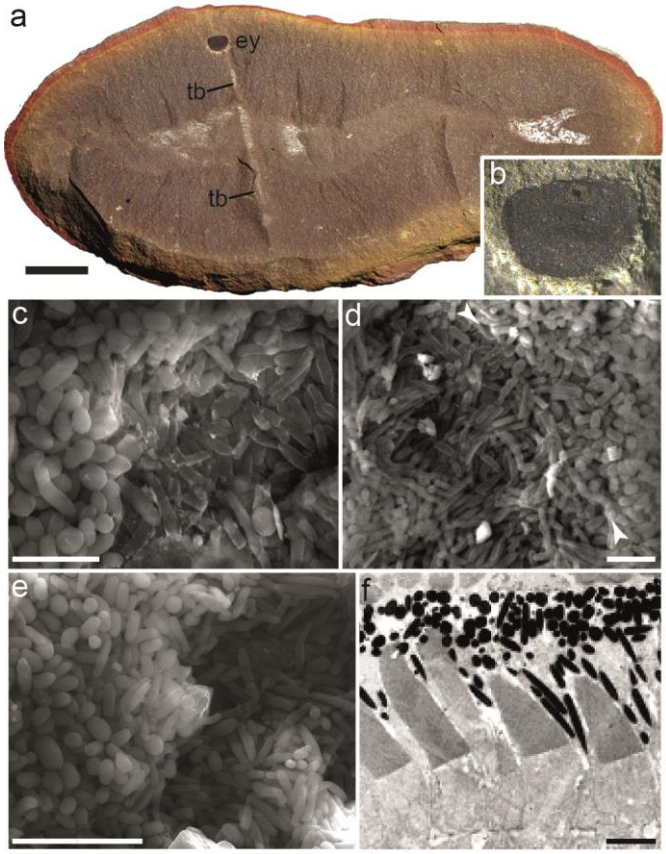

Figure 2 | The ultrastructural details of the eyes of *Tullimonstrum gregarium* from the Mazon Creek Lagerstätte and an extant anchovy (*Coilia nasus*). **a,** *Tullimonstrum* (PE22061) with eye (ey) and transverse bar (tb). **b,** Eye in **a**, with possible lens (l) (see Extended Data Fig. 1). **c - e,** Back-scattered electron SEM images of melanosomes in *Tullimonstrum* eye (**c**, **d**, PE22061; **e**, PE22126). White arrows indicate the boundary between the layers of melansomes with different morphologies. **f,** Radial TEM cross section larval anchovy retina with oblate and cylindrical melanosomes in the retinal pigment epithelium (dark pigment granules). Image used with permission[29]. Decay induced collapse of the RPE would result in a fossilised structure with cylindrical and oblate melanosome morphologies overlying each other as seen in **c** - **e** (see Extended Data Fig. 1). Scale bars: **a**, 10 mm; **c - f** 2 µm.

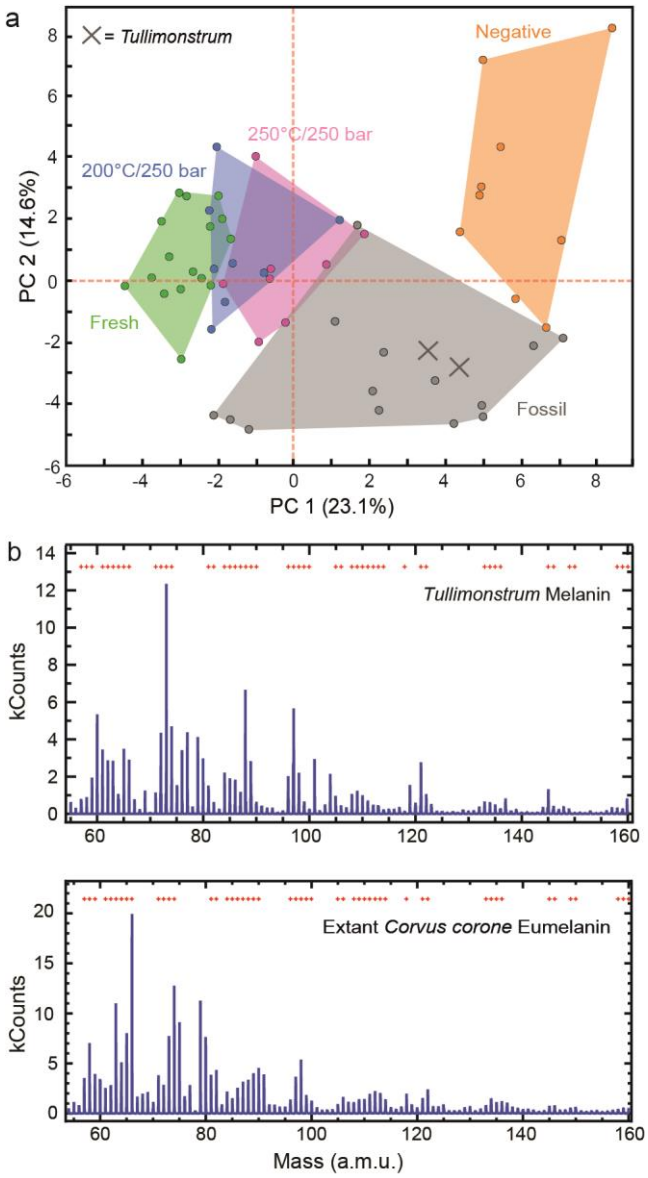

Figure 3 | TOF-SIMS analysis of melanosomes preserved in *Tullimonstrum gregarium*. **a**, Principal components analysis of 55 negative secondary ion peaks[28] from fresh, artificially matured (24 hours at: 200˚C/250 bar and 250˚C/250 bar) and fossil melanin samples as well as a variety of known melanin-negative samples. Two melanin samples from the eye of *Tullimonstrum* (BMRP2014MCP1000) are marked as 'X's. Two separately acquired spectra from regions of the eye in *T. gregarium* reveal spectra (**b**) with similar relative intensity distributions of the melanin-specific peaks as extant melanin samples (e.g. extant crow melanin). However, the PCA analysis indicates that fresh and fossil melanins are quantifiably different. Artificially matured melanins plot closer to fossil samples, which suggests

diagenetic alteration of fossil melanin[28]. The *T. gregarium* spectrum is most similar to that from an Eocene frog eye as well as a lamprey eye from Mazon Creek (See Extended Data Figs 3, 4 and 6 for loadings and details). Red crosses in **b** indicate eumelanin characteristic fragments.

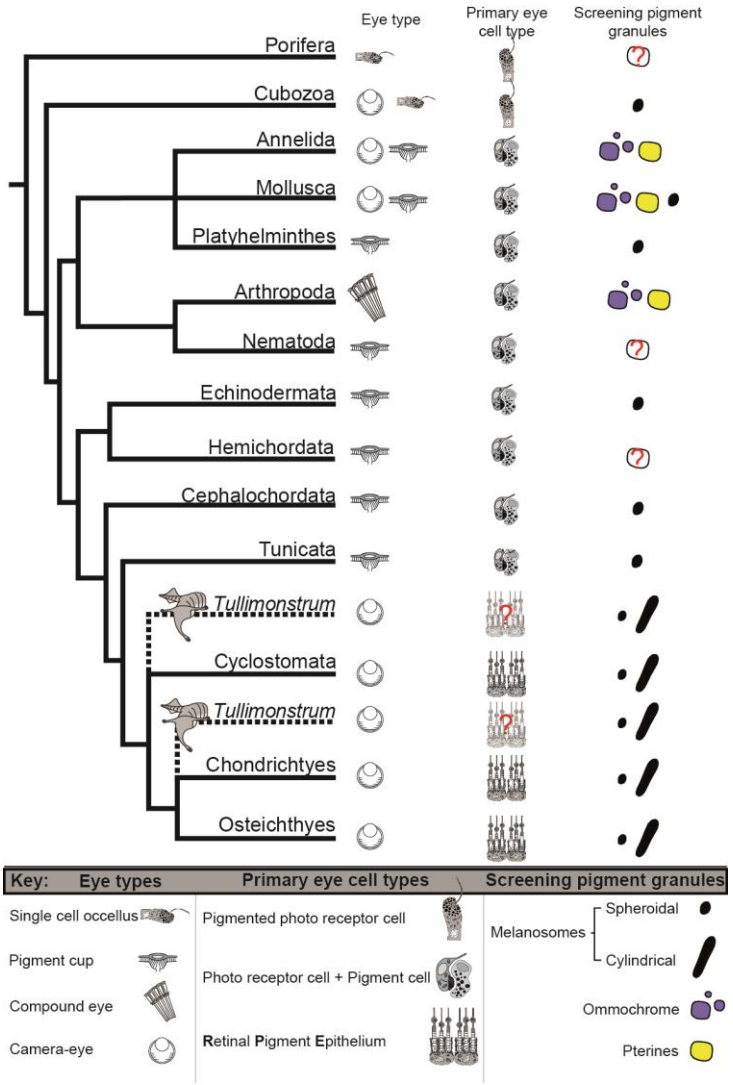

Figure 4 | The phylogenetic distribution of photoreceptor organs, cell architecture and pigment granule chemistry and morphology in animals. Vertebrates are unique among eye-bearing metazoans in having their screening pigment cells and photoreceptors in separate tissues (RPE and the rods and cones layer; although as seen in Fig. 2f the RPE layer may project in between the rods and cones). In all other metazoans these cells interfinger to form a retinal layer, or are combined into a single cell in basal metazoans and

some protostomes. Possible positions of *Tullimonstrum* within total group vertebrates are indicated. For further details see supplementary information.

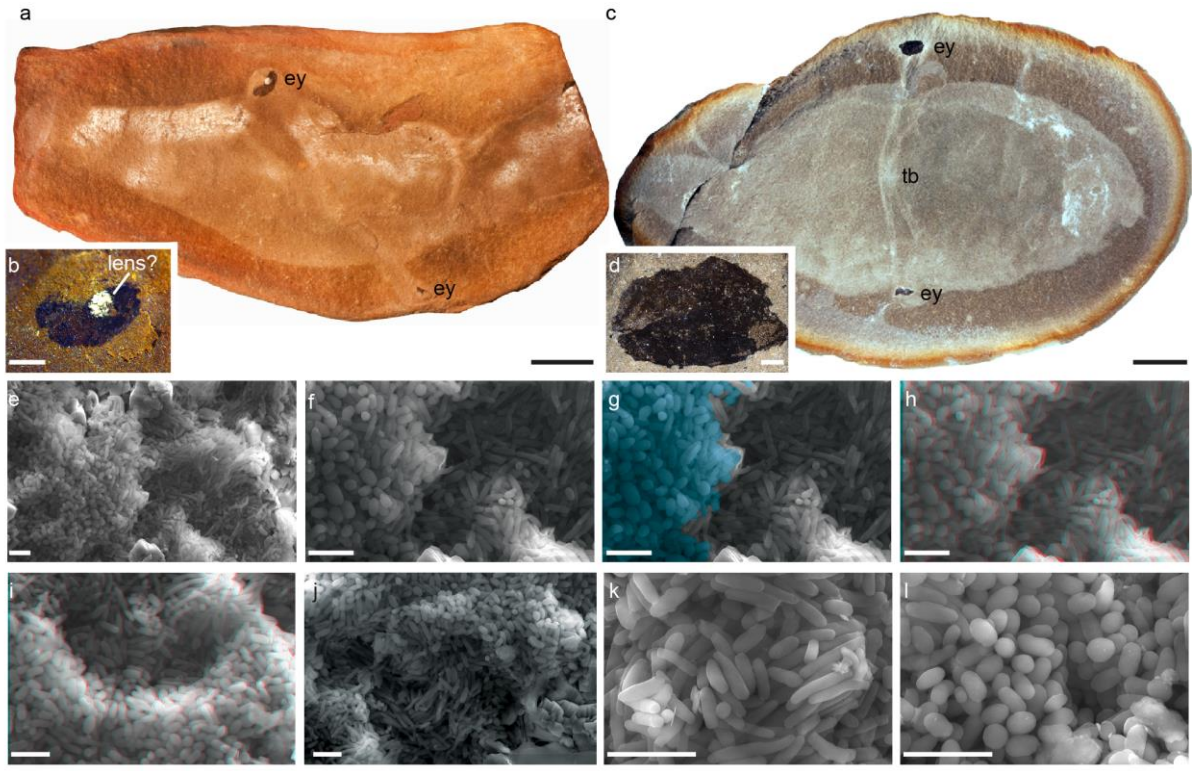

Extended Data Figure 1: Details of *Tullimonstrum gregarium* eyes. a, complete specimen (MCPX27C5369 - BMNH) with eyes (ey). Scale bar: 10 mm. **b**, close-up of the uppermost eye in **a**, showing dark carbonaceous material and an approximately centrally-positioned white circular area with high relief. The white mineral is kaolinite. This is similar to the eye in *Bandringa* (Extended Data Fig. 5) and the white infilling of kaolinite may be indicative of a lens[15]. Scale bar: 1 mm. **c-l** Specimen PE22126 (FMNH)**. c,** complete specimen in nodule showing clearly defined eyes (ey) and transverse bar (tb). Scale bar: 10 mm. **d,** the uppermost eye in **c**. Scale bar: 1 mm. **e-l** SEM images of the eye ultrastructure. **e**, oblate melansomes on the left hand side and underlying cylindrical melanomes on the right hand side. **f-h** are higher magnification images of the centre of **e;** in **g,** oblate melanosomes are highlighted in blue, and **h** is an anaglyph (3D) of the same field of view as

f and **g** (see also Fig. 2). **i,** anaglyph (3D) image showing oblate melansomes overlying cyclindrical melansomes. **j**, oblate and cyclindrical melansomes in distinct layers; **k** and **l** show the cylindrical and oblate melanosome morphologies, respectively. Scale bars: 2 µm.

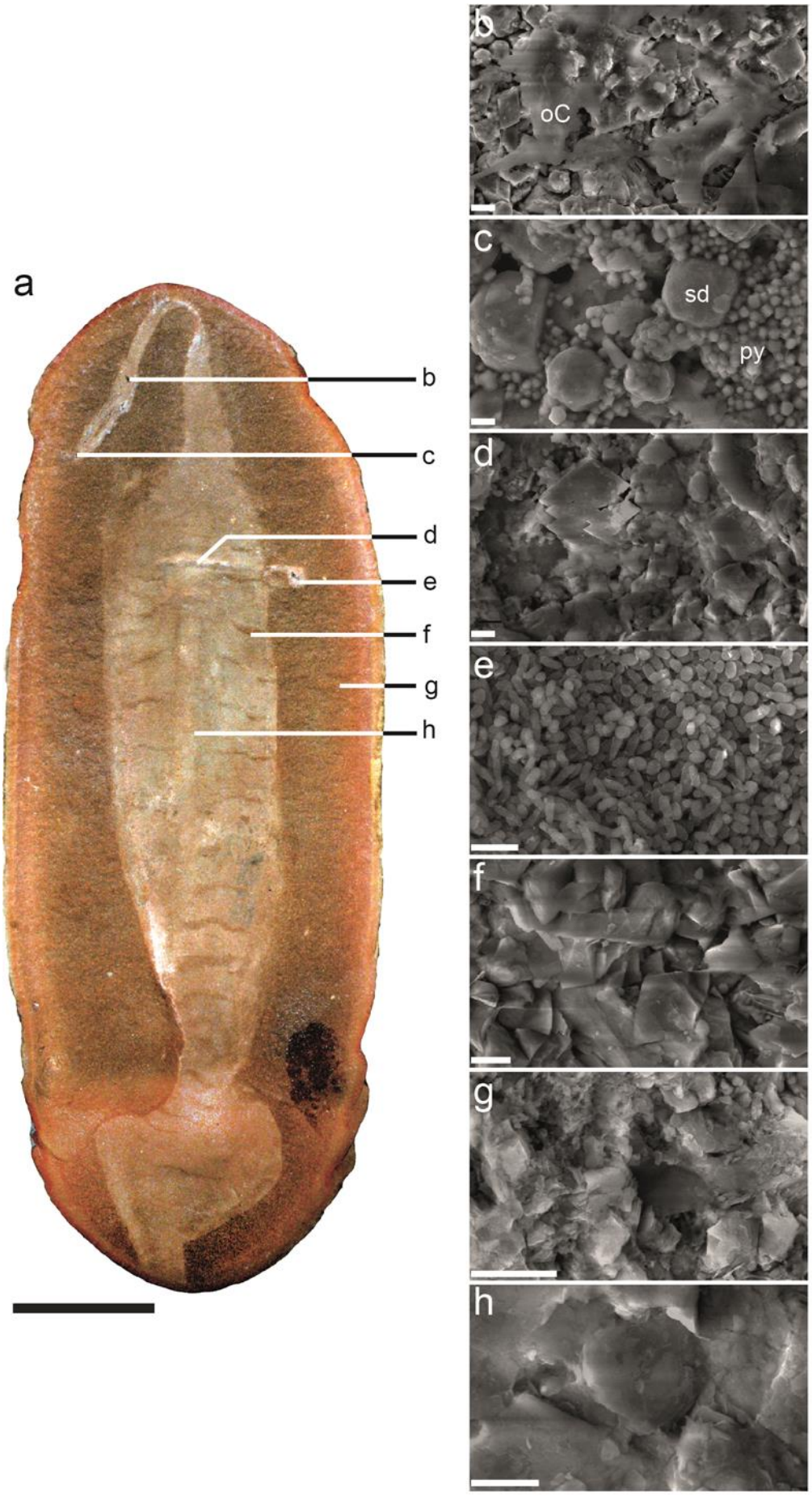
a
b
c
d
e
f
g
h
oC
sd
py

Extended Data Figure 2: *Tullimonstrum* (BMRP2014MCP1000) with SEM images of anatomical features. a, complete specimen (anterior at top) with anatomical features labelled (see Fig. 1) and accompanying SEM images showing their preservation to demonstrate that *only* the eyes exhibit melansomes. Scale bar: 10 mm. **b**, proboscis with small, dark, organic carbon patch (oC) which has a smooth texture; **c**, distal portion of the proboscis 'claw' showing pyrite crystals and framboids; **d**, eye bar containing siderite cements and clay minerals; **e**, eye showing melansome texture; **f**, dark transverse bands (?myomeres) containing mainlyb siderite; **g**, the nodule matrix, siderite and detrital clay minerals; **h**, main trunk, siderite and clay minerals. oC: organic carbon; sd: siderite; py: pyrite. Scale bars: 2 µm.

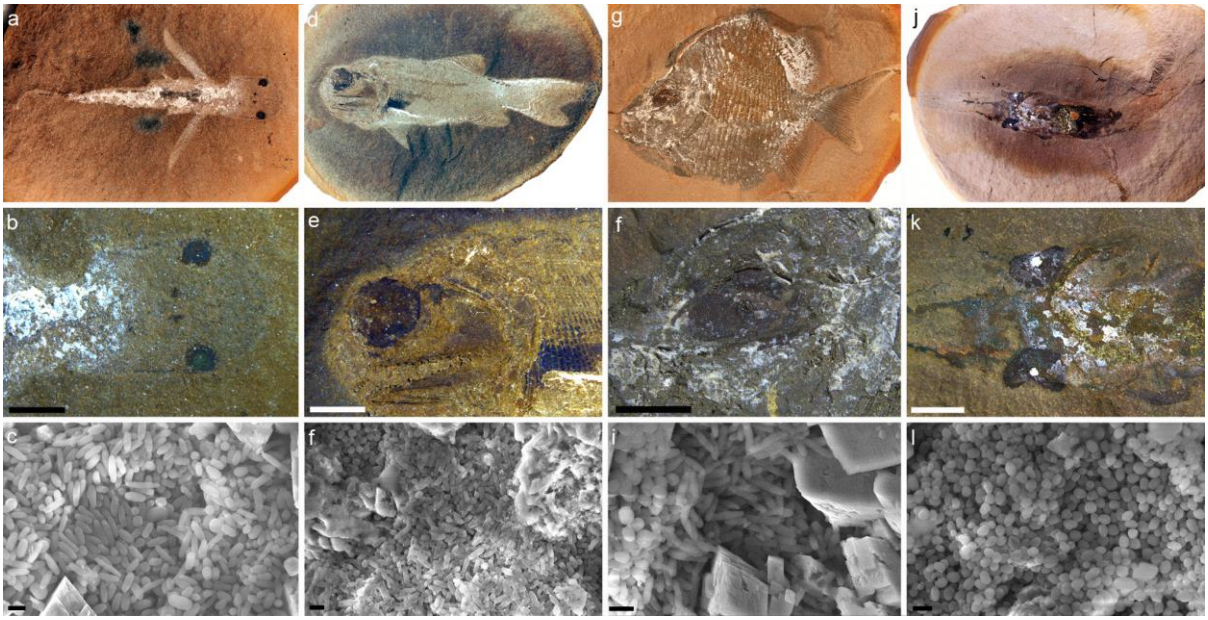

Extended Data Figure 5: Gnathostomes with dark eyes and eye ultrastructure from the Mazon Creek Lagerstätte. a-c *Esconicthys apopyris* (PF9831) a putative larval lungfish[18]. **d-f** *Elonichthys peltigerus* (ROM56794). **g-i** *Platysomus circularis* (PF7333)**. j-l** *Bandringa rayi* (ROM56789) - note the white centrally-positioned circular feature in both eyes. The white mineral is kaolinite and this most likely reflects the position of the lens[15]. **c,f,i,l** are BSE-SEM images of the eyes from each corresponding fossil. Melanosomes of cylindrical

and oblate morphologies are found in *Esconicthys, Elonichthys* and *Platysomus;* in *Bandringa* only oblate melanosomes occur. Scale bars for **b,e,h,k**: 5 mm. Scale bars for **c,f,i,l**: 1 µm.

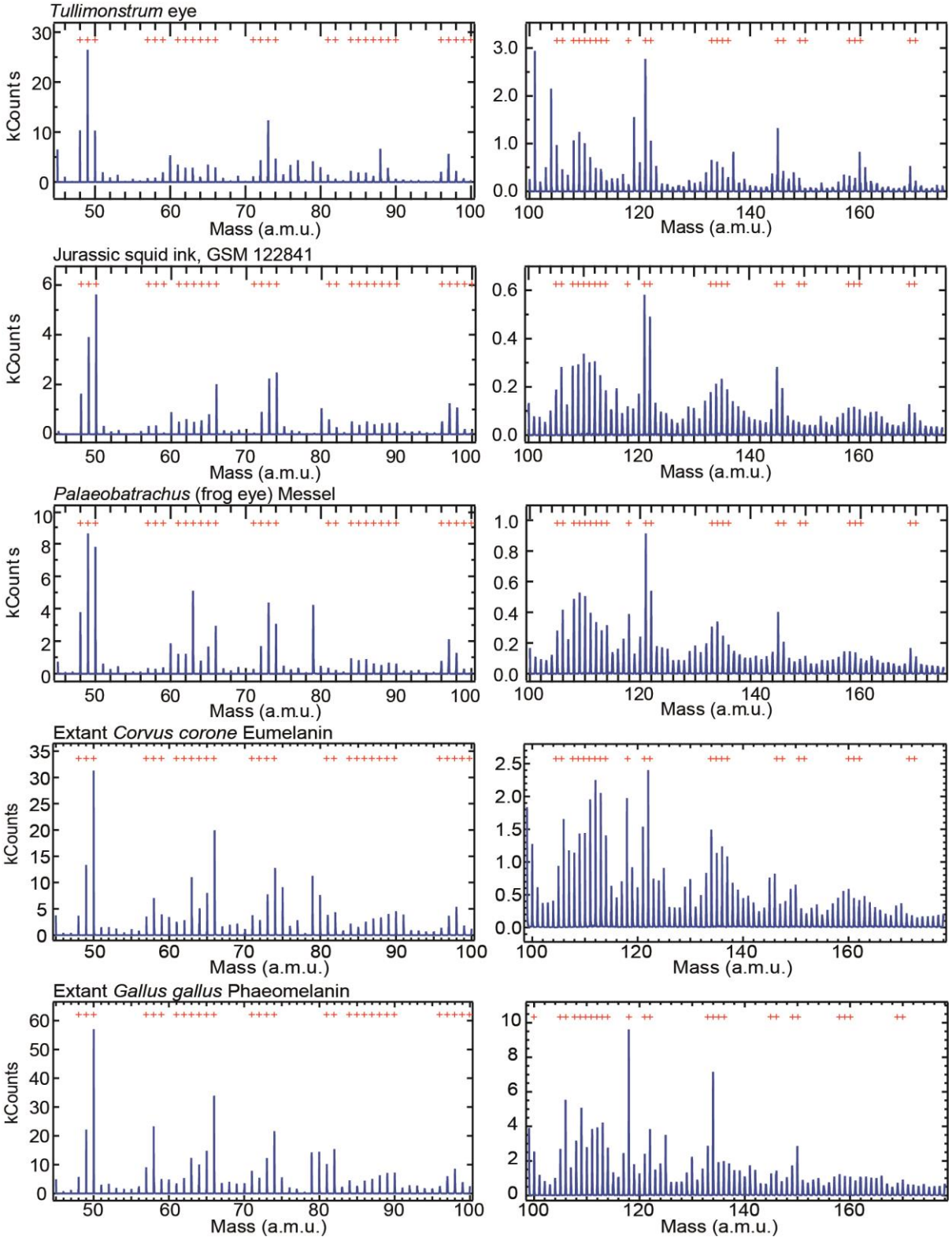

Extended Data Figure 4: Negative ion TOF-SIMS spectra in the 45-100 and 100-175 atomic mass unit range. For comparison to the *T. gregarium* eye melanosomes, spectra from an Eocene frog eye from Messel is shown along with a Jurassic ink sac from Lyme

Regis. Two extant melanin samples are also shown from a glossy black Carion Crow (*Corvus corone*) and a reddish brown domestic chicken (*Gallus gallus*). (Comparative spectra are from Colleary *et al.*[13]). Negative ion TOF-SIMS spectra in the 45-100 a.m.u range are shown in the left column and 100-175 a.m.u range in the right column.

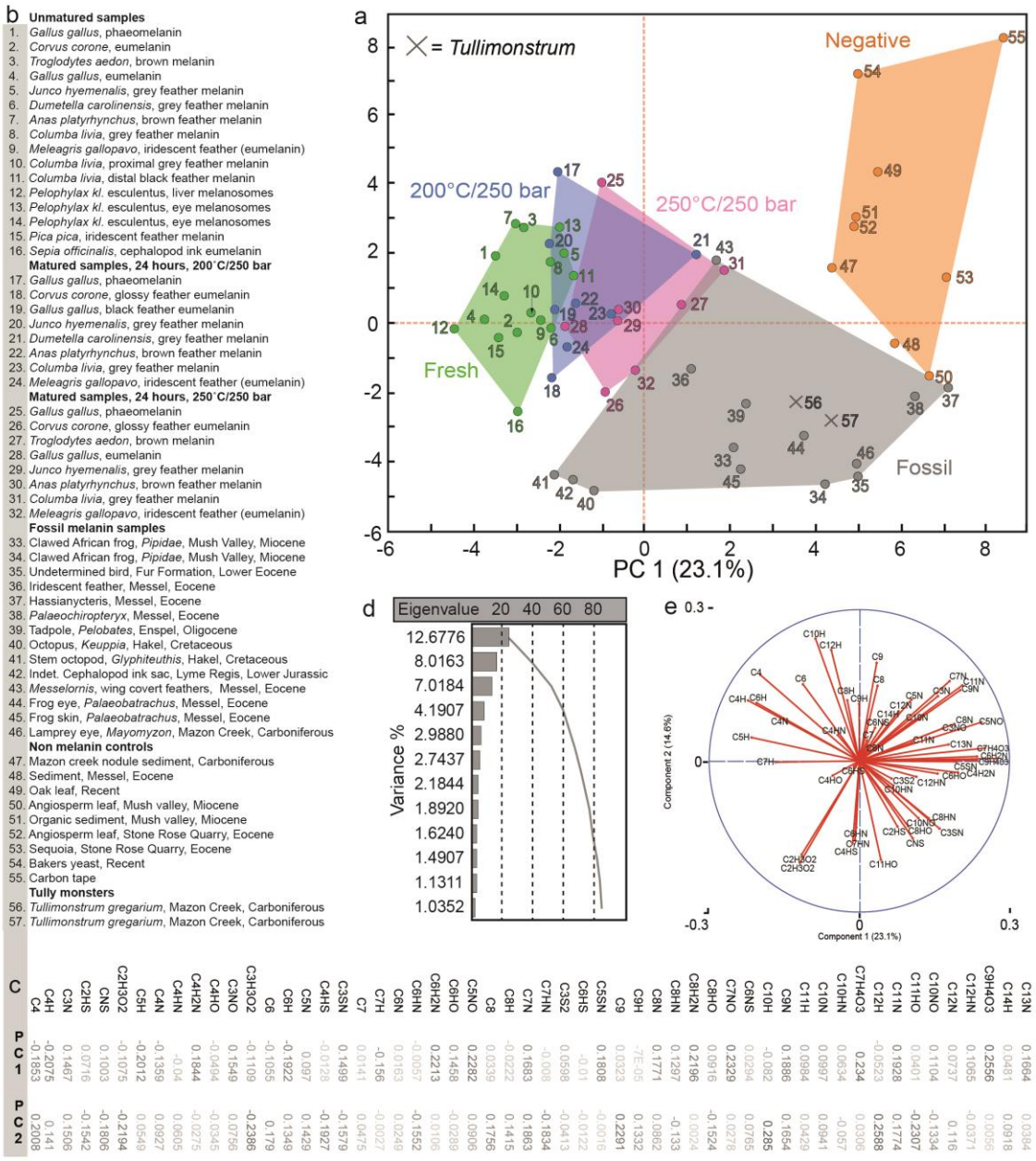

Extended Data Figure 3: Principal Components Analysis of TOF-SIMS spectra: a, PCA plot of 55 negative secondary ion peaks[28] from fresh, artificially matured (24 hours at: 200˚C/250 bar and 250˚C/250 bar) and fossil melanin samples as well as a variety of melanin negative samples, and samples from *Tullimonstrum* eye (listed in **b**). The two separately acquired spectra from regions of the eye in *Tullimonstrum* have similar relative intensity distributions of the melanin-specific peaks as other fossil melanosome samples, plotting near to an Eocene frog eye, and a lamprey eye from Mazon Creek. **c**, Eigenvectors delineating the principal component (PC) axes 1 and 2 in the initial coordinate system

defined by the melanin-specific fragments. **d**, Eigenvalues in decreasing order for the first 12 eigenvectors obtained through PCA. **e**, Loading plot showing the projections of the initial coordinate system onto the PC 1 and 2 axes. Fragments such as C_nNH-, C_nNO-, C_nNS-, C_nSH- and C_nOH- are mostly responsible for the separation of fossil melanin in the PCA space, whereas fragments such as C_n- and C_nH- separate the fresh melanin. This indicates both the chemical degradation (loss of carbon, nitrogen, sulphur and water) and structural degradation (loss of weaker molecular bonding) of melanin during the fossilisation process.

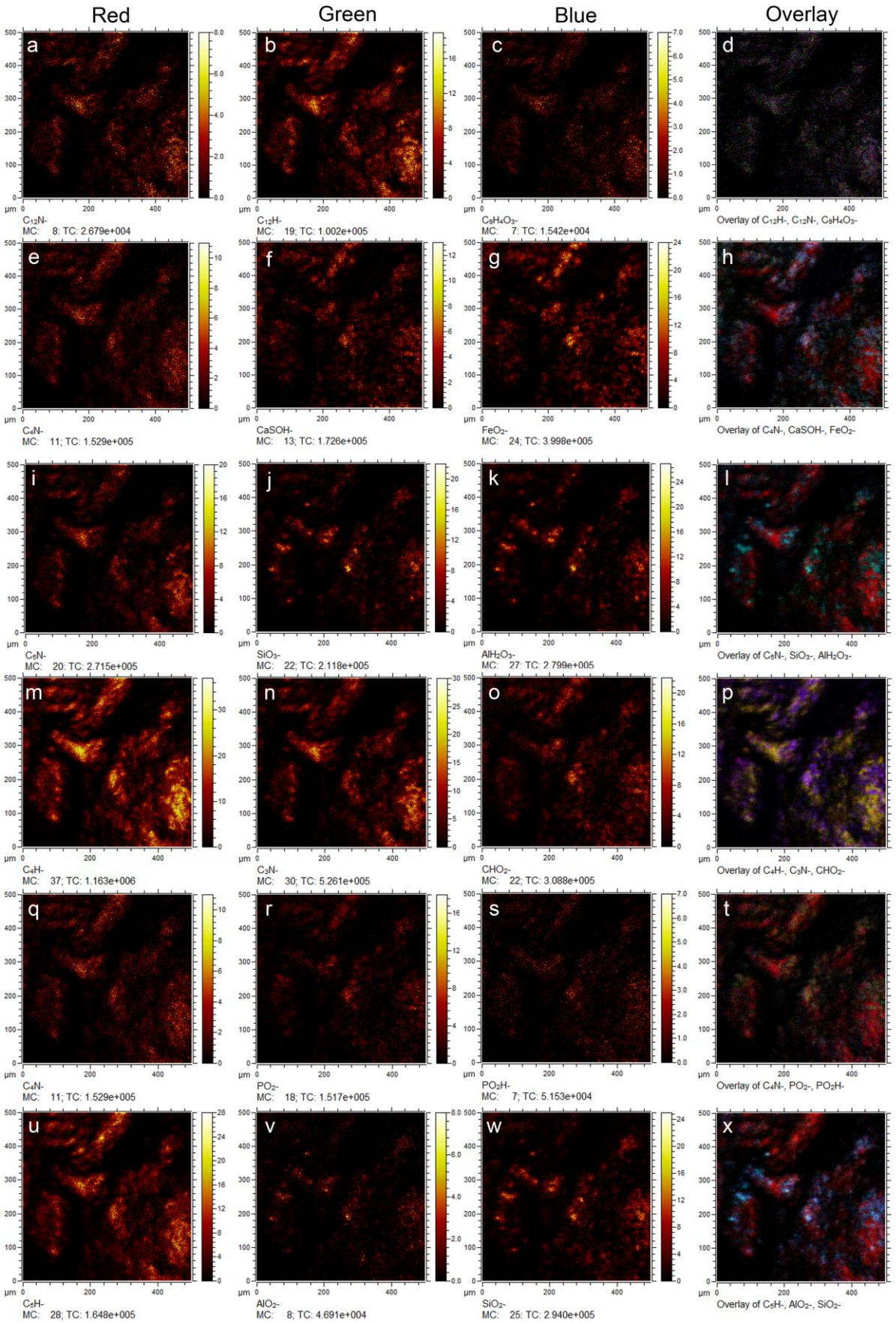
Red
Green
Blue
Overlay
a
b
c
d
C12N-
MC: 8; TC: 2.679e+004
C12H-
MC: 19; TC: 1.002e+005
C9H4O3-
MC: 7; TC: 1.542e+004
Overlay of C12H-, C12N-, C9H4O3-
e
f
g
h
C4N-
MC: 11; TC: 1.529e+005
CaSOH-
MC: 13; TC: 1.726e+005
FeO2-
MC: 24; TC: 3.998e+005
Overlay of C4N-, CaSOH-, FeO2-
i
j
k
l
C5N-
MC: 20; TC: 2.715e+005
SiO3-
MC: 22; TC: 2.118e+005
AlH2O3-
MC: 27; TC: 2.799e+005
Overlay of C5N-, SiO3-, AlH2O3-
m
n
o
p
C4H-
MC: 37; TC: 1.163e+006
C3N-
MC: 30; TC: 5.261e+005
CHO2-
MC: 22; TC: 3.088e+005
Overlay of C4H-, C3N-, CHO2-
q
r
s
t
C4N-
MC: 11; TC: 1.529e+005
PO2-
MC: 18; TC: 1.517e+005
PO2H-
MC: 7; TC: 5.153e+004
Overlay of C4N-, PO2-, PO2H-
u
v
w
x
C5H-
MC: 28; TC: 1.648e+005
AlO2-
MC: 8; TC: 4.691e+004
SiO2-
MC: 25; TC: 2.940e+005
Overlay of C5H-, AlO2-, SiO2-

Extended Data Figure 6 : TOF-SIMS intensity maps from eye region in *Tullimonstrum*, showing relative distribution of ions derived from melanin relative inorganic ions from the matrix.

False colour chemical mapping of the spatial distribution of several melanin-specific secondary ion fragments (**a, e, i, m, q, u**) compared to the maps of melanin characteristic ions (**b, c, n, o**) and inorganic ions derived from the sediment (SiOn-: **j, w**, Al(Hn)On- : **k, v**) and the concretion cements (FeO2-: **g**, CaSOH-: **f**), which map distinctly from the melanin ions or co-occur with melanin (PO2-: **r**, PO2H-: **s**). The secondary ion CHO2-, is a likely secondary ion from carboxyl groups (**o**) and is a known constituent of melanin. It is observed that is exhibits only a moderate overlap with melanin markers (**p**), which could be attributed to different diagenetic alterations of the melanin or some difference in composition. The right hand column maps are composites of the tentatively assigned secondary ions in their respective row (i.e. **d** is a composite of **a** – **c**). The distribution of inorganic and organic ions shows that the melanin and matrix ions are distinct contributions to the TOF SIMS spectrum, as seen in Extended data Fig. 4.